Chemosphere 309 (2022) 136727

Contents lists available at ScienceDirect

Chemosphere

journal homepage: www.elsevier.com/locate/chemosphere

Effect of steel slag on ammonia removal and ammonia-oxidizing microorganisms in zeolite-based tidal flow constructed wetlands

Yuhuan Zou [a,b,c], Yongqiang Yang [a,b,*], Shijun Wu [a,b], Fanrong Chen [a,b], Runliang Zhu [a,b]

[a] CAS Key Laboratory of Mineralogy and Metallogeny & Guangdong Provincial Key Laboratory of Mineral Physics and Materials, Guangzhou Institute of Geochemistry, Chinese Academy of Sciences, 511 Kehua Street, Guangzhou, 510640, China
[b] CAS Center for Excellence in Deep Earth Science, 511 Kehua Street, Guangzhou, 510640, China
[c] University of Chinese Academy of Sciences, 19 Yuquan Road, Beijing, 100049, China

HIGHLIGHTS

- NH_4^+-N removal rate was improved by adding steel slag in zeolite-based TFCW.
- Higher NH_4^+-N removal rate was attributed to the neutral pH maintained by steel slag.
- Steel slag addition increased the diversity and abundance of AOMs.
- Steel slag addition shifts the dominant *amoA* genes from AOB to CAOB in the TFCWs.

GRAPHICAL ABSTRACT

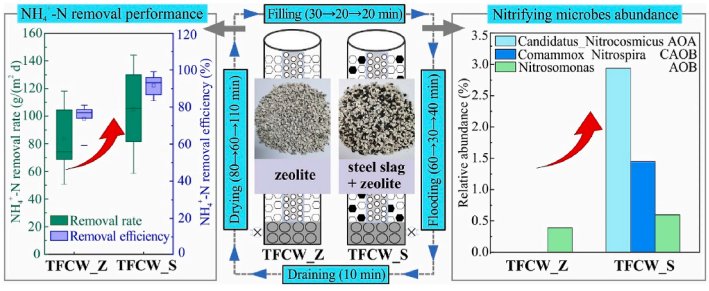

ARTICLE INFO

Handling editor: A ADALBERTO NOYOLA

Keywords:
Tidal flow constructed wetlands
Steel slag
Hydraulic loading rate
Comammox *Nitrospira*
amoA

ABSTRACT

The ammonia removal performance of tidal flow constructed wetlands (TFCWs) requires to be improved under high hydraulic loading rates (HLRs). The pH decrease caused by nitrification may adversely affect the NH_4^+–N removal and ammonia-oxidizing microorganisms (AOMs) of TFCWs. Herein, TFCWs with zeolite (TFCW_Z) and a mixture of zeolite and steel slag (TFCW_S) were built to investigate the influence of steel slag on NH_4^+-N removal and AOMs. Both TFCWs were operated under short flooding/drying (F/D) cycles and high HLRs (3.13 and 4.69 $m^3/(m^2\ d)$). The results revealed that a neutral effluent pH (6.98–7.82) was achieved in TFCW_S owing to the CaO dissolution of steel slag. The NH_4^+-N removal efficiencies in TFCW_S (91.2 ± 5.1%) were much higher than those in TFCW_Z (73.2 ± 7.1%). Total nitrogen (TN) removal was poor in both TFCWs mainly due to the low influent COD/TN. Phosphorus removal in TFCW_S was unsatisfactory because of the short hydraulic retention time. The addition of steel slag stimulated the flourishing AOMs, including *Nitrosomonas* (ammonia-oxidizing bacteria, AOB), *Candidatus_Nitrocosmicus* (ammonia-oxidizing archaea, AOA), and comammox *Nitrospira*, which may be responsible for the better ammonia removal performance in TFCW_S. PICRUSt2 showed that steel slag also enriched the relative abundance of functional genes involved in nitrification (*amoCAB*, *hao*, and *nxrAB*) but inhibited genes related to denitrification (*nirK*, *norB*, and *nosZ*). Quantitative polymerase chain reaction (qPCR) revealed that complete AOB (CAOB) and AOB contributed more to the *amoA* genes in TFCW_S and TFCW_Z, respectively. Therefore, this study revealed that the dominant AOMs could be significantly changed in zeolite-

* Corresponding author. CAS Key Laboratory of Mineralogy and Metallogeny & Guangdong Provincial Key Laboratory of Mineral Physics and Materials, Guangzhou Institute of Geochemistry, Chinese Academy of Sciences, 511 Kehua Street, Guangzhou, 510640, China.
E-mail address: yqyang@gig.ac.cn (Y. Yang).

https://doi.org/10.1016/j.chemosphere.2022.136727
Received 6 June 2022; Received in revised form 7 September 2022; Accepted 30 September 2022
Available online 6 October 2022
0045-6535/© 2022 Elsevier Ltd. All rights reserved.

based TFCW by adding steel slag to regulate the pH in situ, resulting in a more efficient NH_4^+–N removal performance.

1. Introduction

Since the 1990s, tidal-flow constructed wetlands (TFCWs) have been gaining attention because of their excellent oxygen supply (Chand et al., 2022; Pang et al., 2015). TFCWs are alternately filled with wastewater and drained, and thus the wastewater acts as a passive pump to expel oxygen-depleted air and draw fresh air into the system (Ju et al., 2014). The current guiding theory for ammonia removal in TFCWs is as follows: NH_4^+ is first adsorbed onto the substrates during the flooding phase and nitrified during the drying phase using drawn atmospheric oxygen (Chang et al., 2014). Therefore, the drawn atmospheric oxygen, rather than the dissolved oxygen in the wastewater, affects the ammonia removal performance, especially for systems with short flooding times. Theoretically, 1 L of the drained effluent is displaced by an equal volume of fresh air, supplying ~280 mg of oxygen at 20 °C (Zhang et al., 2021). This oxygen supply is proportional to the hydraulic loading rates (HLRs) of TFCWs, thus achieving an efficient and low-cost oxygen supply.

Due to the excellent NH_4^+ adsorption capacity, zeolite is an ideal substrate for TFCWs (Ji et al., 2022; Zhang et al., 2021). Zeolite-based TFCWs outperformed active carbon- and ceramsite-based TFCWs in removing NH_4^+–N and TN (Liu et al., 2014; Xu et al., 2022). Adding 10% zeolite significantly increased NH_4^+–N removal of the gravel-based TFCW at an HLR of 3 $m^3/(m^2\ d)$ (Zhang et al., 2021). However, a significant decrease in effluent pH owing to strong nitrification was observed in TFCWs (Chang et al., 2014; Zhang et al., 2021). The acidic environment induced by nitrification may be detrimental to further ammonia removal via ammonia-oxidizing microorganisms (AOMs) since most are more suitable for neutral or slightly alkaline environments (Grunditz and Dalhammar, 2001; Lu et al., 2020). Employing alkaline substrates may be a feasible approach.

Steel slag is a highly efficient substrate for phosphorus removal, owing to its high alkalinity and Ca content (Barca et al., 2013; Hua et al., 2016; Zuo et al., 2018). Slag-based CWs with a long hydraulic retention time (HRT) usually lead to a high effluent pH (≥9) due to excessive CaO-slag dissolution (Barca et al., 2013; Xu et al., 2019), which might be detrimental to microbes involved in nitrogen removal. Moreover, using steel slag alone as a substrate in TFCWs is less effective due to its weak adsorption capacity for NH_4^+. Employing a mixture of steel slag and zeolite in TFCWs may alleviate substrate acidification and thus achieve more efficient ammonia removal performance. However, the NH_4^+ adsorption capacity of zeolite is seriously inhibited by steel slag because of the excess release of OH^- and Ca^{2+} with long contact times (Shi et al., 2017). The effluent pH was ~7.5 in a steel slag-based TFCW with a flooding time of 3 h (Saeed et al., 2020). Therefore, we presumed that a short flooding time and high HLRs might result in a slight increase in effluent pH, which may be conducive to the removal of ammonia by AOMs, hence deserving further investigation.

Ammonia oxidation is mediated by ammonia-oxidizing archaea (AOA) and bacteria (AOB) (Konneke et al., 2005). Recently, complete AOB (CAOB) affiliated with *Nitrospira* lineage II, capable of independently performing complete nitrification, was discovered, adding a vital process to microbial ammonia removal (Daims et al., 2015). The diversity, adaptation, and evolution of AOMs in the soil are potentially driven by pH (Gubry-Rangin et al., 2011). In a TFCW filled with zeolite and steel slag in sequence and with effluent recirculation, AOB was significantly greater in the steel slag layer than in the zeolite layer, whereas it is unclear whether AOA and CAOB exist in this system (Cao et al., 2022). Therefore, the effect of a mixture of steel slag and zeolite on AOMs in TFCWs needs further investigation.

In this study, two laboratory-scale TFCWs, filled with zeolite and the mixture of zeolite and steel slag, respectively, were constructed outdoors to treat low C/N sewage at high HLRs (3.13 and 4.69 $m^3/(m^2\ d)$). The objectives of this study were to (1) investigate the influence of steel slag addition on the effluent pH and pollutant removal performance of TFCWs, (2) reveal the microbial community and nitrifying functional genes using 16S rRNA gene sequencing and quantitative polymerase chain reaction (qPCR) techniques, respectively, and (3) investigate the functional genes involved in nitrogen transformation using PICRUSt2 based on the Kyoto Encyclopedia of Genes and Genomes (KEGG) database.

2. Materials and methods

2.1. Lab-scale TFCWs description and operation

Two laboratory-scale TFCWs were constructed using identical polyvinyl chloride columns (length = 120 cm and inner diameter = 10.2 cm). As shown in Fig. 1a, the bottom layers were filled with 10 cm deep gravel (20–30 mm), while the upper treatment layers were filled with zeolite (3–5 mm) alone in TFCW_Z, and a mixture of zeolite (3–5 mm) and steel slag (2–4 mm) (volume ratio = 3:2) in TFCW_S, both having a height of 100 cm and 36% porosity. Zeolite and steel slag were purchased from the Zhejiang and Henan provinces of China. The chemical composition and mineral phases of zeolite have been reported in a previous study (Zhang et al., 2021). The steel slag was characterized by X-ray fluorescence (XRF) and X-ray diffraction (XRD); detailed information is provided in the Supporting Information. The tidal operation (feeding-flooding-draining-drying) was produced by peristaltic pumps and electromagnetic valves controlled by time controllers. It should be noted that plants were not involved in this study, mainly to eliminate their influence at different growth stages on nitrogen removal (Zhang et al., 2021).

The experiment lasted for almost 12 months, from November 2019 to October 2020, and included three phases based on the operating conditions after the start-up phase. The flooding/drying (F/D) cycles in phases I, II, and III were 1.5 h/1.5 h, 0.83 h/1.17 h, and 1 h/2 h, respectively (Fig. 1b). During stable operation phases, the daily average temperatures were above 15 °C. Both TFCWs were not pre-inoculated

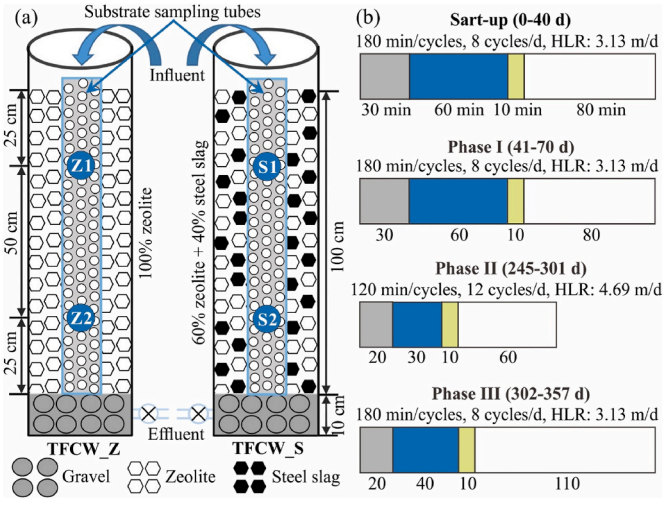

Fig. 1. Schematic diagram of the experiment equipment (a) and operating conditions within a cycle during different phases (b). Gray, blue, green, and white represent the feeding, flooding, draining, and drying periods, respectively.

and fed directly with actual domestic sewage. Sewage collected from sewage pipes in a residential area in Guangzhou was intermittently pumped into the TFCWs after about two days of sedimentation. The characteristics of the sewage in different phases are summarized in Table 1.

2.2. Sampling and analysis

Water samples collected periodically from the influent and effluent were analyzed for pH, chemical oxygen demand (COD), NH_4^+–N, total phosphorus (TP), NO_2^-–N, and NO_3^-–N according to the standard methods issued by State Environmental Protection Administration (SEPA) of China. The solution pH was analyzed using a pH meter (PB-10, Sartorius), whereas others were analyzed using spectrophotometric methods with a UV–Vis spectrophotometer (755B, Jinghua, China). Total nitrogen (TN) was calculated as the sum of NO_2^-–N, NO_3^-–N, and NH_4^+–N. The maximum P adsorption capacity of the steel slag was determined using isotherm batch experiments (Supporting Information).

2.3. Microbial sample collection and analysis

At the end of phase II, four biofilm samples labeled Z1, Z2, S1, and S2 (Fig. 1a) were collected from the TFCWs. Universal primers (515FmodF and 806 RmodR) targeting the 16S rRNA gene V4 region were used to amplify the 16S rRNA genes (Wang et al., 2020). The nitrification-related genes (including ammonia monooxygenase encoding genes (*amoA*) of AOB, AOA, CAOB, and nitrite oxidoreductase encoding gene (*nxrA*)) were characterized by qPCR with specific PCR primer sets (Table S1). The detailed methods of high-throughput sequencing and qPCR are described in a previous study (Zhang et al., 2021).

PICRUSt2, an emerging bioinformatics tool, was used to predict nitrogen metabolism based on high-throughput sequencing data (Douglas et al., 2020). The sequencing data were first annotated using the KEGG database using the online Majorbio Platform (www.Majorbio.com). Subsequently, the output results were analyzed and visualized using the R software (v 4.0.5).

2.4. Statistical analysis

The microbial community data were analyzed using the Majorbio cloud platform (https://cloud.majorbio.com/). One-way analysis of variance with Tukey's test was performed to compare the difference in performance between the two TFCWs using SPSS software (version 18.0). A *p*-value below 0.05 was considered statistically significant.

3. Results and discussion

3.1. Treatment performance of TFCWs

3.1.1. Ammonia removal

As Table 1 presents, the average NH_4^+–N concentrations in TFCW_Z effluent were 13.7, 7.26, and 6.31 mg/L in phases I, II, and III with the corresponding NH_4^+–N removal efficiencies of 61.3, 76.1, and 77.8%, respectively. In contrast, the effluent NH_4^+–N concentrations in TFCW_S were consistently less than 5 mg/L (Fig. 2a), and the corresponding NH_4^+–N removal efficiencies were 97.3, 92.4, and 86.1%, respectively. In phase II, higher ammonia removal rates (ARRs) were achieved with 108.6 and 132.0 g/(m^2 d) for TFCW_Z and TFCW_S, respectively. In general, TFCW_S filled with steel slag and zeolite achieved significantly higher NH_4^+–N removal efficiency than TFCW_Z filled with zeolite alone ($p < 0.05$).

The results in phases II and III indicated that a longer drying time (110 min) failed to promote NH_4^+–N removal. A drying time of 60 min was sufficient to oxidize the adsorbed NH_4^+–N. Similarly, Liu et al. (2020) found that the NH_4^+–N removal efficiency of an SC-AA-TFCW slightly increased from 80 to ~85% as the drying time increased from 60 to 120 min, whereas it drastically decreased to 47% when the drying time was reduced to 30 min. Therefore, using a drying time of 60 min in TFCWs may be feasible for removing NH_4^+–N from domestic sewage when suitable substrates are employed. The drying time setting was mainly determined by the time required for the nitrifiers to oxidize ammonia, which is related to the abundance and activity of the nitrifiers and the total amount of the adsorbed ammonia. However, when treating wastewater with higher concentrations of NH_4^+-N (>80 mg/L), a short drying time might fail to remove NH_4^+–N efficiently. For example, even with a long F/D cycle of 8/4 h, zeolite-steel slag-TFCW removed only 70.9% of NH_4^+–N with an influent NH_4^+–N of 87.95 mg/L (Cao et al.,

Table 1
Characteristics of influent and effluent (mean) and removal performance (mean) of the TFCWs during the experimental period.

Parameters	Start-up			Phase I			Phase II			Phase III		
	Influent	Effluent		Influent	Effluent		Influent	Effluent		Influent	Effluent	
		TFCW_Z	TFCW_S		TFCW_Z	TFCW_S		TFCW_Z	TFCW_S		TFCW_Z	TFCW_S
pH	7.61	7.02	7.85[f]	7.46	6.42	7.37[f]	7.67	6.07	7.61[f]	7.50	5.44	7.17[f]
NH_4^+–N (mg/L)	31.2	12.4	3.97	35.4	13.7	0.97	30.4	7.26	2.26	28.7	6.31	3.99
ARRs[a] (g/(m^2 - d))	–	58.7	85.1	–	67.9	107.8	–	108.6	132.0	–	70.2	77.4
RE[b] (%)	–	60.0	87.2[f]	–	61.3	97.3[f]	–	76.1	92.4[f]	–	77.8	86.1[f]
NO_3^-–N (mg/L)	0.64	3.20	9.31	< LOD[e]	16.1	27.4	< LOD	20.7	20.4	< LOD	21.7	21.5
NO_2^-–N (mg/L)	< LOD	5.32	18.48	< LOD	2.45	1.46	< LOD	0.11	0.07	< LOD	0.06	0.08
COD (mg/L)	80.7	34.8	38.4	89.8	32.8	20.9	97.8	40.0	34.0	99.8	43.3	40.4
CRRs[c] (g/(m^2 d))	–	143.6	132.3	–	178.4	215.6	–	271.0	299.0	–	176.9	185.9
RE (%)	–	56.2	54.1	–	63.5	76.8[f]	–	59.2	65.3[f]	–	56.3	59.6
TN (mg/L)	31.8	20.9	31.8	35.7	32.2	29.9	30.5	28.1	22.8	28.8	28.1	25.6
NRRs[d] (g/(m^2 d))	–	34.1	0.22	–	10.8	18.1	–	11.2	36.2	–	2.19	10.2
RE (%)	–	33.8	1.15	–	9.76	16.3	–	7.13	25.2[f]	–	2.31	11.2
COD/TN	2.54	–	–	2.52	–	–	3.24	–	–	3.50	–	–
TP (mg/L)	2.81	1.63	1.81	3.06	2.61	2.14	2.80	2.63	2.09	2.61	2.58	2.02
RE (%)	–	40.6	34.9	–	14.8	30.2[f]	–	6.05	25.2[f]	–	0.71	22.4[f]

[a] NH_4^+–N removal rates.
[b] Removal efficiency.
[c] COD removal rates.
[d] Total nitrogen removal rates.
[e] Below limit of detection.
[f] Indicate statistically significant differences from TFCW_Z ($p < 0.05$).

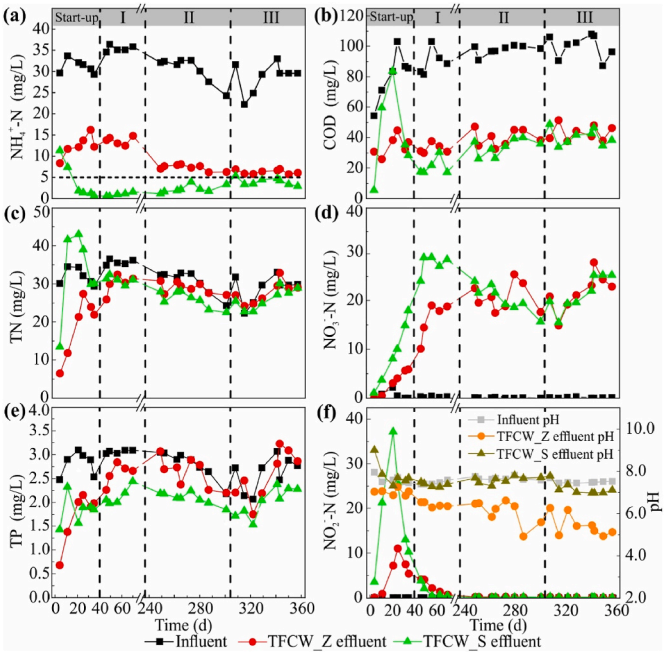

Fig. 2. Treatment performance and pH level of the TFCWs during the experimental period: (a) NH_4^+–N, (b) COD, (c) total nitrogen (TN), (d) NO_3^-–N, (e) total phosphorus (TP), and (f) NO_2^-–N and pH. The dashed line in (a) indicates the NH_4^+–N concentration of 5 mg/L.

2022); another possible reason for the low ammonia removal may be that the high ammonia in the influent was not fully adsorbed by the substrates and flowed out with the effluent. Therefore, the NH_4^+-N removal performance of TFCWs in treating wastewater with high NH_4^+-N is worthy of further study.

The ARRs are usually below 3 g/(m^2 d) in conventional CWs and less than 10 g/(m^2 d) in intensified CWs (Fan et al., 2013; Vymazal, 2007), whereas much higher ARRs (10–58 g/(m^2 d)) are achieved in TFCWs (Tan et al., 2019; Wang et al., 2017; Zhang et al., 2021). Because of the high HLR (4.69 m^3/(m^2 d)) and substrate optimization, the NH_4^+–N removal performance of this study outperformed that of previous investigations. It is noteworthy that TFCWs still have great potential for improving ARRs, for example, further optimizing substrate composition and enhancing HLRs by adding packing depth.

3.1.2. COD removal

The average influent COD concentration was 93.1 ± 11.6 mg/L with a C/N ratio of 3.03 during the monitoring period, which was recognized as low C/N sewage. As presented in Table 1, the average COD removal efficiencies of the TFCWs were between 56.3 and 76.8% in phases I, II, and III, and the effluent concentrations were always less than 50 mg/L. Furthermore, TFCW_S performed better than TFCW_Z in phases I and II ($p < 0.05$). Organic matter in TFCWs can be removed by aerobic and anaerobic processes (Chang et al., 2014). The temporally averaged profile of COD during a typical F/D cycle of 72 h (36-h feeding phase, 35.75-h flooding phase, and 15-min draining phase) showed that most of the COD were removed within 4 h due to rapid aerobic degradation (Li et al., 2019). Aerobic degradation usually plays a more critical role in COD removal in TFCWs because of the extensive aerobic/anoxic conditions (Chang et al., 2014), especially in systems with a long feeding phase. However, in TFCWs with short feeding times, anaerobic degradation via denitrification may contribute more to organic removal because of the more robust anoxic/anaerobic environment. The effect of feeding time on COD removal via aerobic or anaerobic pathways requires further study.

Similar to NH_4^+–N, the maximum COD removal rates (CRRs) were also achieved in phase II with 271.0 and 299.0 g/(m^2 d) for TFCW_Z and TFCW_S, respectively. In contrast, TFCWs with high influent COD concentrations (>290 mg/L) achieved higher removal efficiencies (>80%) but lower CRRs (<200 g/(m^2 d)) due to the relatively low HLRs (<0.7 m^3/(m^2 d)) (Hu et al., 2012; Wang et al., 2017), indicating that longer F/D cycles and lower HLRs might be conducive to COD removal.

3.1.3. Total nitrogen removal

As shown in Fig. 2d and Table 1, NO_3^-–N was the dominant product of nitrification in phases I, II, and III, with concentrations between 10.1 and 28.9 mg/L. Consequently, TN removal efficiencies were usually less than 25%. In phase II, the TN removal efficiency of TFCW_S (25.2%) was much higher than that of TFCW_Z (7.13%) ($p < 0.05$). In phase III, the lowest TN removal efficiency was obtained in TFCW_S and TFCW_Z, suggesting that a long drying phase may be disadvantageous for denitrification. Zhang et al. (2021) found that short drying times (50 and 80 min) were more favorable for TN removal than a long drying time (140 min) when treating low-strength wastewater. TFCWs achieved higher TN removal with an F/D cycle of 5/1 h than 3/3 h when treating wastewater with 30.7 mg/L TN; however, the opposite result was obtained when treating wastewater with 61.5 mg/L TN (Chang et al., 2014). Therefore, the influent concentration should be considered when setting F/D cycles in TFCWs.

Although various TN removal pathways (ammonia volatilization, plant uptake, denitrification, and anammox, etc.) exist in TFCWs, denitrification plays a leading role in nitrogen removal (Chang et al., 2014; Saeed et al., 2020). During the flooding period, denitrifiers used influent organic matter to remove NO_3^-–N produced during the last drying period. The influent C/N ratio is a key factor affecting TN removal in TFCWs. For instance, TN removal efficiency increased by 24%–30% when the C/N ratio rose from 2.9 to above 5.0 (Roth et al., 2021). With an increase in the C/N ratio from 4 to 12, the TN removal efficiency increased from 50 to 82% (Zhi and Ji, 2014). In this study, the low TN removal efficiency could be ascribed to the low influent C/N ratio (2.24–4.07).

Various strategies have been employed to improve TN removal in TFCWs, including effluent recirculation (Cao et al., 2022; Pang et al., 2022), microbial fuel cells enhancement (Tang et al., 2021), and biochar-immobilized bacteria (Zhao et al., 2022). However, these strategies increase the operational difficulty and/or energy consumption, and TN removal rates are usually below 30 g/(m^2 d) owing to low HLRs. TN removal performance of TFCWs at high HLRs still needs to be improved.

3.1.4. Variation of pH and phosphorus removal

As shown in Fig. 2f, the effluent pH of TFCW_Z gradually decreased from 6.42 in phase I to 5.44 in phase III, while it fluctuated between 7.17 and 7.61 in TFCW_S. The poor denitrification and H^+ produced by robust nitrification resulted in a low effluent pH in TFCW_Z. By contrast, steel slag steadily released alkalinity through the dissolution of CaO-slag, neutralizing the produced H^+ and maintaining the effluent pH neutral in TFCW_S. Steel slag is well known for its promising performance in phosphorus removal (Barca et al., 2013; Zuo et al., 2018). The primary phosphorus removal mechanism is associated with the dissolution of CaO-slag followed by the precipitation of Ca phosphate (Barca et al., 2013). As shown in Table 1, TP removal efficiencies in TFCW_S were 30.2, 25.2, and 22.4% in phases I, II, and III, respectively, showing a gradually decreasing trend caused by slag exhaustion (Claveau-Mallet et al., 2014). The TP removal efficiency in TFCW_Z decreased from 14.8% in phase I to 0.71% in phase III, which is significantly lower than that in TFCW_S ($p < 0.05$), demonstrating that adding 40% steel slag promotes TP removal.

According to the coefficients of the Langmuir isotherm, the maximum P adsorption capacity of the steel slag was 43.83 mg P/g (Fig. S2), similar to those obtained in previous studies (Table S2). Steel slags with small particle sizes (<1 mm) usually had much higher P adsorption capacity (Table S2). However, TP removal efficiencies in this

study were inferior to those in other studies (Barca et al., 2013; Zuo et al., 2018). TP removal performance improved with increasing CaO content and/or by decreasing the size of the materials (Barca et al., 2013), while high influent phosphorus concentrations and low HRT reduced steel slag longevity (Claveau-Mallet et al., 2014). The CaO content of the slag in this study was lower than that of the basic oxygen furnace slag but higher than that of the electric arc furnace slag (Table S3). Moreover, the HRT was usually above 24 h in previous studies (Barca et al., 2013), which is much longer than in this study. The short HRT and 40% (v/v) addition proportion of slag resulted in a limited CaO release, which was detrimental to TP removal. However, the limited CaO release was beneficial for removing NH_4^+–N because of the suitable pH. Therefore, the inconsistency of HRT requirements makes it difficult to remove NH_4^+–N and TP simultaneously in TFCW_S.

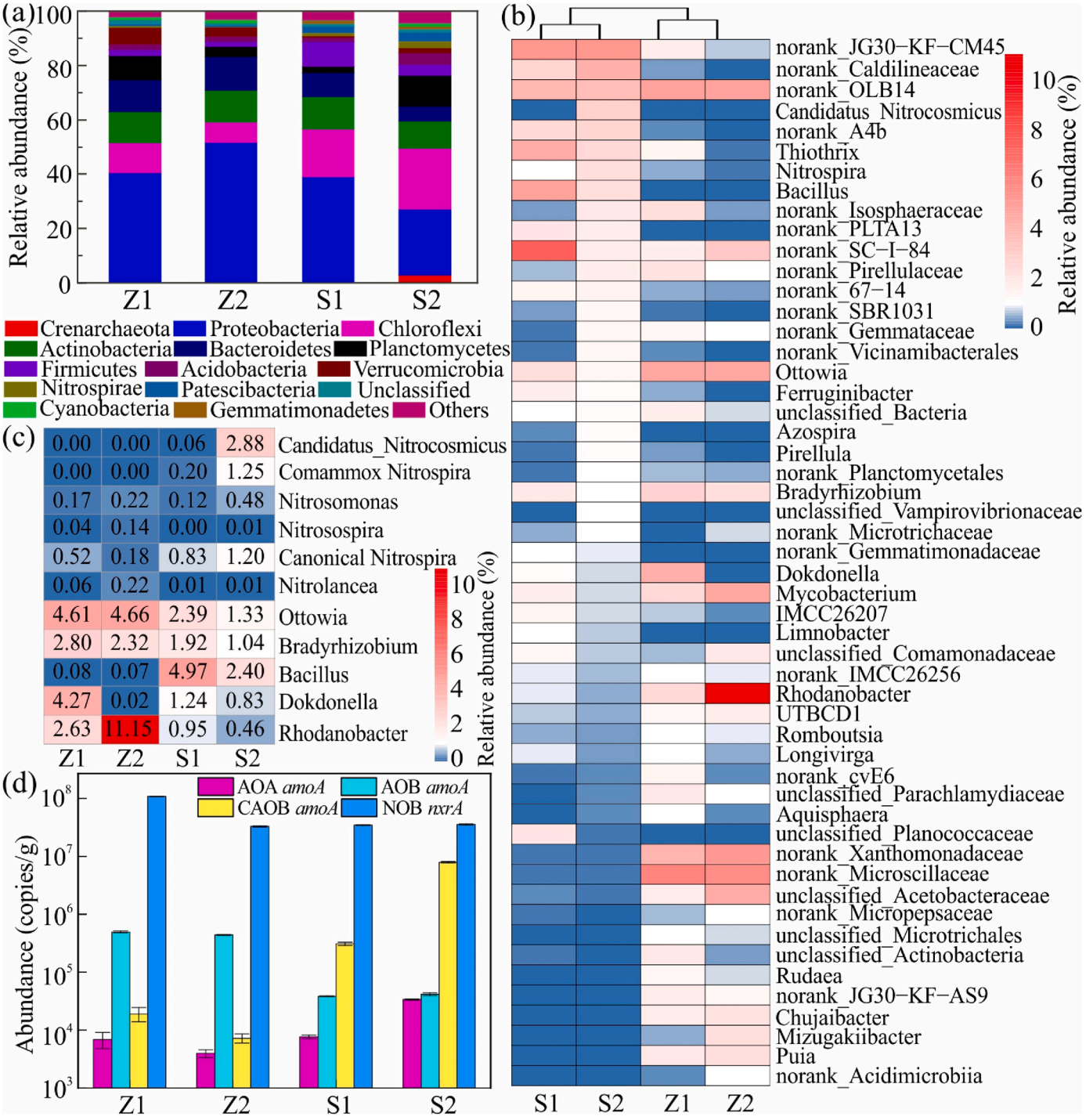

Fig. 3. Microbial community structure of the four biofilm samples in the TFCWs at (a) phylum and (b) genus levels (relative abundance >1% at least in one sample); (c) Heat map of potential nitrifying and denitrifying microorganisms in the TFCWs (Numbers in the heat map indicate the percentage of relative abundance); (d) Abundances of functional genes involved in nitrification in the TFCWs. Z1, Z2, S1, and S2 represent the samples collected from the upper and lower layers in TFCW_Z and TFCW_S, respectively.

3.2. Microbial community and diversity

3.2.1. Microbial community composition at phylum and genus levels

As Table S4 shows, S1 and S2 exhibited higher microbial diversity and richness (Shannon, ACE, and Chao1) than Z1 and Z2, suggesting that the mixture of steel slag and zeolite provide more appropriate conditions for bacteria to flourish, potentially resulting in higher nitrogen removal in TFCW_S. As shown in Fig. 3a, the predominant phylum was *Proteobacteria* (46.02 and 31.53%), closely related to nitrogen transformation. In addition, *Nitrospirae* exhibited a higher relative abundance in TFCW_S (1.75%) than in TFCW_Z (0.35%), whereas *Crenarchaeota* was only detected in TFCW_S, especially in S2 (2.89%). The first isolated nitrifier (*Nitrosopumilus maritimus* SCM1) was affiliated with the phylum *Crenarchaeota* (Konneke et al., 2005).

The dominating genera in TFCW_Z were *Rhodanobacter* (6.89%), *norank_Microscillaceae* (5.93%), *norank_OLB14* (4.86%), *norank_Xanthomonadaceae* (4.73%), and *Ottowia* (4.63%), whereas they were *norank_JG30*-KF-*CM45* (5.35%), *norank_SC-I-84* (4.53%), *norank_OLB14* (3.84%), *Bacillus* (3.68%), and *Thiothrix* (3.54%) in TFCW_S (Fig. 3b and Table S5). *Rhodanobacter* has been identified as a denitrifier preferring low-pH environments (Prakash et al., 2012; Zhan et al., 2020), exhibiting higher abundances in Z1 (2.64%) and Z2 (11.15%) than in S1 and S2 (<1.0%), which could be ascribed to the different pH environment in the two TFCWs. As shown in Fig. 3c, a variety of widely reported denitrifying bacteria were detected in TFCW_Z and TFCW_S, including *Ottowia*, *Bradyrhizobium*, *Bacillus,* and *Dokdonella* (Huang et al., 2020; Pishgar et al., 2019; Spring et al., 2004). Although denitrifiers were enriched in both TFCWs, the TN removal performance was heavily restricted owing to the low influent C/N ratio.

3.2.2. Relative abundances of CAOB and the canonical nitrifiers

Candidatus_Nitrocosmicus, belonging to *Crenarchaeota*, was detected in S1 (0.06%) and S2 (2.88%) (Fig. 3c), suggesting that AOA may be involved in NH_4^+–N removal in TFCW_S. A similar phenomenon was also observed in two-stage TFCWs with effluent pH slightly above 7 (Pang et al., 2022). AOA outperformed AOB and CAOB, contributing more to ammonia oxidation in wastewater treatment plants (WWTPs) in the cold season (Pan et al., 2018). AOB (*Nitrosomonas* and *Nitrosopira*) with low abundance (<0.5%) were also detected in TFCW_Z and TFCW_S, which is consistent with previous studies (Fu et al., 2020; Han et al., 2019; Li et al., 2021b). Su et al. (2018) found that AOB activity was independent of its abundance, which may be why high NH_4^+–N removal performance can still be achieved in TFCW_Z.

Nitrolancea, the first example of NOB in the phylum *Chloroflexi* (Sorokin et al., 2018), had low proportions in both TFCWs (0.01–0.22%). *Nitrospira* was the main NOB, with relative abundances of 0.52, 0.18, 1.03, and 2.45% in Z1, Z2, S1, and S2, respectively. In addition, phylogenetic analysis revealed that *Nitrospira* OTU924 and OTU2573 were classified as *Ca. Nitrospira inopinata* and *Ca. Nitrospira nitrosa*, whereas OTU749 was affiliated with *Nitrospira defluvii*, an isolated nitrite-oxidizing strain (Fig. S3).

As shown in Fig. 3c, comammox *Nitrospira*, AOA, and AOB coexisted in TFCW_S, whereas only AOB was identified in TFCW_Z. The synergistic interaction of these different AOMs may be responsible for the improved NH_4^+–N removal in TFCW_S. The absence of CAOB in TFCW_Z could be ascribed to the low effluent pH (<6.0), as comammox *Nitrospira* favors growth in slightly alkaline soils (Xu et al., 2020). CAOB outnumbered other nitrifiers in TFCW and WWTPs with relatively low-strength NH_4^+–N (Roots et al., 2019; Zhang et al., 2021), while they were undetected or accounted for a small proportion in WWTPs with medium- and high-strength ammonia (Gonzalez-Martinez et al., 2016). However, CAOB is active and abundant in both copiotrophic and oligotrophic terrestrial ecosystems (Li et al., 2022), suggesting whether ammonia concentration shapes niche differentiation between CAOB and other AOMs remains to be investigated.

3.3. Functional prediction analysis by PICRUSt2

As shown in Fig. 4a, metabolism at pathway level 1 (77.2–78.0%) contributed more to the total relative abundance, in line with that in domestic wastewater (Dai et al., 2021). At level 2 (Fig. 4b), global and overview maps (40.0%), carbohydrate metabolism (8.7%), amino acid metabolism (8.0%), and energy metabolism (4.5%) were the main metabolic pathways, which were closely related to microbial growth and survival (Li et al., 2021a).

To further reveal nitrogen metabolism in TFCWs, the key enzyme genes that participate in nitrification, denitrification, assimilatory and dissimilatory nitrate reduction (ANR and DNR) were investigated using PICRUSt2. Genes associated with nitrification were widespread in the TFCWs and had higher abundances in TFCW_S (Fig. 4c). For instance, *amoA* coding for ammonia monooxygenase was 1.74 times as abundant in TFCW_S than in TFCW_Z. Genes (*nirK*, *norB,* and *nosZ*) related to denitrification significantly outnumbered the nitrification genes, especially in TFCW_Z. Genes encoding the nitrite reductase (NADH) large and small subunits (*nirB* and *nirD*) were the predominant nitrogen transformation genes, consistent with a previous study (Sun et al., 2021). Therefore, the mixture of steel slag and zeolite may be beneficial for the enrichment of nitrification genes but not for denitrification genes, which is consistent with the results of nitrifiers and denitrifiers.

3.4. Functional genes associated with nitrification

AOA *amoA* gene always showed lower abundance than AOB and CAOB *amoA* genes (Fig. 3d). The copy numbers of AOB *amoA* were 4.99×10^5 and 4.43×10^5 copies/g in Z1 and Z2, respectively, which was significantly higher than AOA and CAOB *amoA*, suggesting that AOB *amoA* might contribute more to ammonia oxidation in TFCW_Z. In contrast, CAOB *amoA*, with abundances of 3.11×10^5 and 7.99×10^6 copies/g in S1 and S2, respectively, outnumbered AOA and AOB *amoA*. Therefore, steel slag affected the distribution of AOMs *amoA* genes, resulting in the predominance of CAOB *amoA* in TFCW_S. CAOB *amoA* genes have been detected in different ecosystems, including agricultural soil, intertidal zone, drinking water systems, and activated sludge (Zhao et al., 2019). In eight WWTPs, the copy numbers of CAOB *amoA* were 2.81×10^9 copies/g, prevailing over AOB *amoA* (Wang et al., 2018). However, Pan et al. (2018) found that CAOB *amoA* was much less abundant than AOA and AOB *amoA* in most of the 23 WWTPs. The key factors affecting the abundance of the CAOB, AOB, and AOA *amoA* genes should be further investigated. The *nxrA* gene presented the highest abundance in all samples (3.29×10^7–1.08×10^8 copies/g) and differed little between the two TFCWs, indicating that it is less affected by steel slag.

3.5. Significance

The key to NH_4^+–N removal in TFCWs is to ensure that ammonia can be adsorbed on the substrate during the flooding time and create a suitable pH for nitrifiers during the drying time, both of which are related to substrates. As shown in Table 2, the ammonia removal performance of ceramsite and active carbon is inferior to that of zeolite and active alumina. Alum sludge and biochar showed efficient nitrogen removal at relatively low HLRs. Compared with previous studies, our study achieved much higher NH_4^+–N removal efficiencies and ARRs, mainly owing to the synergy of zeolite to adsorb ammonia and steel slag to release alkalinity. However, it should be noted that the realization of efficient ammonia removal and short F/D cycles in this study are based on the moderate-strength influent ammonia, while its performance in treating wastewater with higher ammonia remains to be investigated. Moreover, this study revealed the specific enrichment of AOA and CAOB and their functional genes in TFCWs filled with zeolite and steel slag, deepening the understanding of AOMs. Overall, this study demonstrates the great potential of the mixture of substrates with strong ammonia

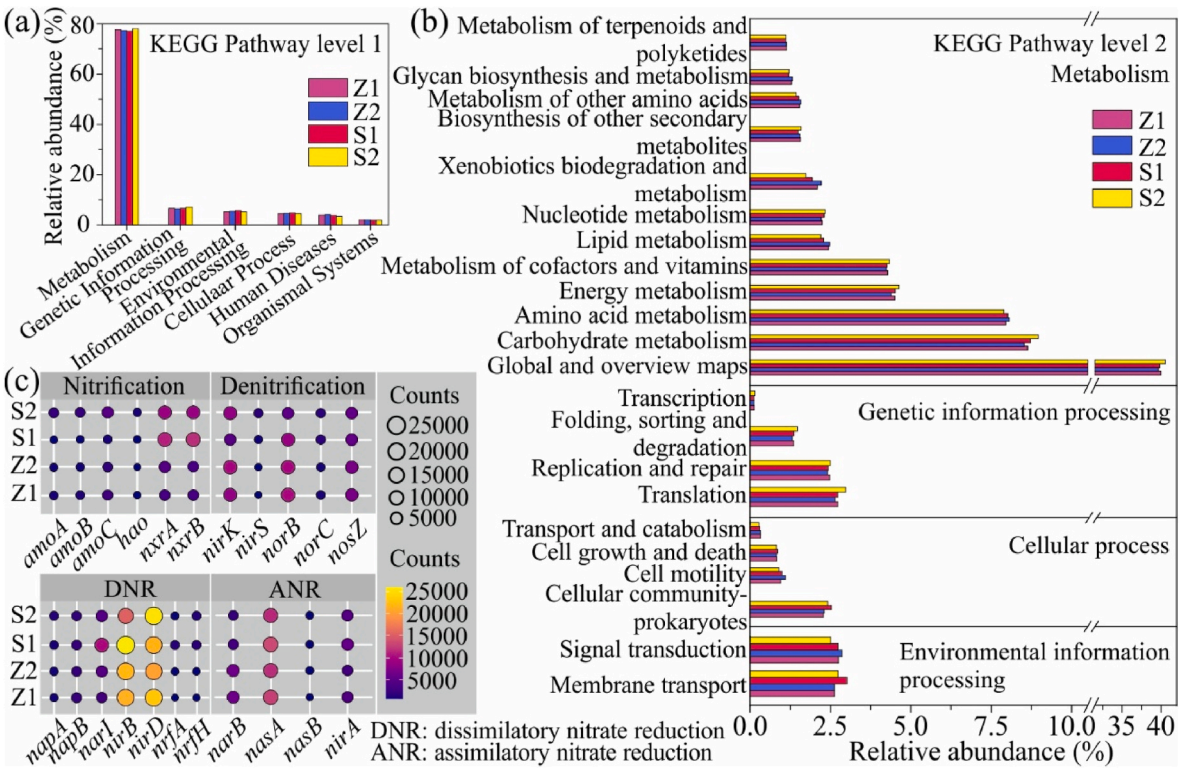

Fig. 4. PICRUSt2 predictions of the functional composition of the biofilm samples. (a) represents the abundance of the KEGG pathway at level 1, (b) the abundance of the main metabolic pathways at level 2, and (c) the counts of predicted functional genes involved in nitrogen metabolism according to KEGG orthology. Z1, Z2, S1, and S2 represent the samples collected from the upper and lower layers in TFCW_Z and TFCW_S, respectively.

Table 2
Operational parameters and removal performance of TFCWs filled with various substrates.

Wastewater type	Substrate type	F/D (h/h)	HLR ($m^3/(m^2\ d)$)	Removal efficiency (%)				ARR[a]	CRR[b]	NRR[c]	References
				NH_4^+–N	COD	TN	TP	($g/(m^2\ d)$)			
Domestic sewage	Zeolite-steel slag (mixed)	0.83/1.17	4.69	92.4	65.3	25.2	25.2	132	299	36.2	This study
Synthetic wastewater	Zeolite-steel slag (layered)	8/4[d]	0.48[e]	70.9	79.9	46.0	–	29.9[e]	37.5[e]	19.8[e]	Cao et al., 2022
Synthetic wastewater	Zeolite-pyrite (layered)	8/4[d]	0.47[e]	58.7	80.3	44.2	–	24.4[e]	36.9[e]	18.6[e]	Cao et al., 2022
Diluted domestic sewage	Zeolite-gravel (mixed)	0.67/2.33	3.0	55.5	37.9	24.0	–	26.72	63.0	11.8	Zhang et al., 2021
Synthetic wastewater	Zeolite	12/12	0.25[e]	89.2	–	75.4	–	15.6[e]	–	14.1[e]	Xu et al., 2022
Synthetic wastewater	Granular active carbon	12/12	0.24[e]	53.7	–	47.1	–	9.0[e]	–	8.4[e]	Xu et al., 2022
Synthetic wastewater	Zeolite	16/8	0.207	97	–	85	–	20.1[e]	–	17.6[e]	Liu et al., 2014
Synthetic wastewater	Biological ceramsite	16/8	0.207	34	–	31	–	7.04[e]	–	6.4[e]	Liu et al., 2014
Domestic wastewater	Biochar	3.5/2.5[d]	0.472	89.8	96.2	82.5	91	22.1[e]	579.7[e]	35.0[e]	Saeed et al., 2020
Diluted swine wastewater	Dewatered alum sludge	5/3	0.44	95	82	85	91	20.9[e]	168.5[e]	23.9[e]	Hu et al., 2014
Synthetic wastewater	Active alumina	4/2	1.35	86.1	85.9	72.8	96.4	57.3[e]	211.5[e]	53.5[e]	Tan et al., 2019
Synthetic wastewater	Shale ceramsite	4/2	1.38	64.9	78.4	47.2	27.5	44.2[e]	193[e]	35.9[e]	Tan et al., 2019

[a] Ammonia removal rate.
[b] COD removal rate.
[c] Total nitrogen removal rate.
[d] Contained sub-cycles.
[e] Calculated according to the data presented in the articles.

adsorption capacity and alkaline substrates to improve ammonia removal in TFCWs, deserving further investigation.

4. Conclusions

The TFCW_S filled with steel slag and zeolite achieved efficient NH_4^+–N removal efficiency (92.4%) and removal rate (132.0 $g/(m^2\ d)$) at an HLR of 4.69 $m^3/(m^2\ d)$, indicating that it is feasible to adopt F/D cycles of 50/70 min in TFCWs to remove NH_4^+–N from the domestic sewage. However, TN removal efficiencies were less than 25%, owing to the low influent C/N ratio. Steel slag addition promoted microbial diversity and richness, resulting in the coexistence of AOA, AOB, and CAOB in TFCW_S, whereas only AOB existed in TFCW_Z. The dominant denitrifiers changed from *Rhodanobacter* and *Ottowia* in TFCW_Z to *Bacillus* in TFCW_S. Furthermore, qPCR results indicated that CAOB and AOB *amoA* were the dominant functional genes of ammonia oxidation in TFCW_S and TFCW_Z, respectively. The neutral pH maintained by the steel slag in TFCW_S was beneficial for hosting AOMs, thereby enhancing ammonia removal. However, the inconsistency in HRT requirements makes it challenging for TFCWs to remove both ammonia

and phosphorus efficiently.

Author contribution statement

Yuhuan Zou: Investigation, Data curation, Methodology, Writing - original draft. **Yongqiang Yang:** Conceptualization, Project administration, Writing - review & editing. **Shijun Wu:** Software, Writing - review & editing. **Fanrong Chen:** Conceptualization, Supervision, Funding acquisition. **Runliang Zhu:** Funding acquisition, Writing - review & editing.

Declaration of competing interest

The authors declare that they have no known competing financial interests or personal relationships that could have appeared to influence the work reported in this paper.

Data availability

The data that has been used is confidential.

Acknowledgments

This work was financially supported by the Fundamental and Applied Fundamental Research Major Program of Guangdong Province, China (2019B030302013) and the Science and Technology Planning Project of Guangdong Province (2017B020236003 and 2020B1212060055). We thank Kangning Ji for his assistance in obtaining relevant experimental materials. This is contribution No. IS-3253 from GIGCAS.

Appendix A. Supplementary data

Supplementary data to this article can be found online at https://doi.org/10.1016/j.chemosphere.2022.136727.

References

Barca, C., Troesch, S., Meyer, D., Drissen, P., Andres, Y., Chazarenc, F., 2013. Steel slag filters to upgrade phosphorus removal in constructed wetlands: two years of field experiments. Environ. Sci. Technol. 47 (1), 549–556. https://doi.org/10.1021/es303778t.

Cao, X., Zheng, H., Liao, Y., Feng, L., Jiang, L., Liu, C., 2022. Effects of iron-based substrate on coupling of nitrification, aerobic denitrification and Fe(ii) autotrophic denitrification in tidal flow constructed wetlands. Bioresour. Technol. 361, 127657 https://doi.org/10.1016/j.biortech.2022.127657.

Chand, N., Kumar, K., Suthar, S., 2022. Enhanced wastewater nutrients in vertical subsurface flow constructed wetland: effect of biochar addition and tidal flow operation. Chemosphere 286, 131742. https://doi.org/10.1016/j.chemosphere.2021.131742.

Chang, Y., Wu, S., Zhang, T., Mazur, R., Pang, C., Dong, R., 2014. Dynamics of nitrogen transformation depending on different operational strategies in laboratory-scale tidal flow constructed wetlands. Sci. Total Environ. 487, 49–56. https://doi.org/10.1016/j.scitotenv.2014.03.114.

Claveau-Mallet, D., Courcelles, B., Comeau, Y., 2014. Phosphorus removal by steel slag filters: modeling dissolution and precipitation kinetics to predict longevity. Environ. Sci. Technol. 48, 7486–7493. https://doi.org/10.1021/es500689t.

Dai, H., Gao, J., Li, D., Wang, Z., Duan, W., 2021. Metagenomics combined with DNA-based stable isotope probing provide comprehensive insights of active triclosan-degrading bacteria in wastewater treatment. J. Hazard Mater. 404 (Pt B), 124192 https://doi.org/10.1016/j.jhazmat.2020.124192.

Daims, H., Lebedeva, E.V., Pjevac, P., Han, P., Herbold, C., Albertsen, M., Jehmlich, N., Palatinszky, M., Vierheilig, J., Bulaev, A., Kirkegaard, R.H., von Bergen, M., Rattei, T., Bendinger, B., Nielsen, P.H., Wagner, M., 2015. Complete nitrification by Nitrospira bacteria. Nature 528 (7583), 504–509. https://doi.org/10.1038/nature16461.

Douglas, G.M., Maffei, V.J., Zaneveld, J., Yurgel, S.N., Brown, J.R., Taylor, C.M., Huttenhower, C., Langille, M.G.I., 2020. PICRUSt2 for prediction of metagenome functions. Nat. Biotechnol. 38, 685–688. https://doi.org/10.1038/s41587-020-0548-6.

Fan, J., Wang, W., Zhang, B., Guo, Y., Ngo, H.H., Guo, W., Zhang, J., Wu, H., 2013. Nitrogen removal in intermittently aerated vertical flow constructed wetlands: impact of influent COD/N ratios. Bioresour. Technol. 143, 461–466. https://doi.org/10.1016/j.biortech.2013.06.038.

Fu, G., Wu, J., Han, J., Zhao, L., Chan, G., Leong, K., 2020. Effects of substrate type on denitrification efficiency and microbial community structure in constructed wetlands. Bioresour. Technol. 307, 123222 https://doi.org/10.1016/j.biortech.2020.123222.

Gonzalez-Martinez, A., Rodriguez-Sanchez, A., van Loosdrecht, M.C.M., Gonzalez-Lopez, J., Vahala, R., 2016. Detection of comammox bacteria in full-scale wastewater treatment bioreactors using tag-454-pyrosequencing. Environ. Sci. Pollut. Res. Int. 23 (24), 25501–25511. https://doi.org/10.1007/s11356-016-7914-4.

Grunditz, C., Dalhammar, G., 2001. Development of nitrification inhibition assays using pure cultures of Nitrosomonas and Nitrobacter. Water Res. 35 (2), 433–440. https://doi.org/10.1016/S0043-1354(00)00312-2.

Gubry-Rangin, C., Hai, B., Quince, C., Engel, M., Thomson, B.C., James, P., Schloter, M., Griffiths, R.I., Prosser, J.I., Nicol, G.W., 2011. Niche specialization of terrestrial archaeal ammonia oxidizers. Proc. Natl. Acad. Sci. U. S. A 108 (52), 21206–21211. https://doi.org/10.1073/pnas.1109000108.

Han, Z., Dong, J., Shen, Z., Mou, R., Zhou, Y., Chen, X., Fu, X., Yang, C., 2019. Nitrogen removal of anaerobically digested swine wastewater by pilot-scale tidal flow constructed wetland based on in-situ biological regeneration of zeolite. Chemosphere 217, 364–373. https://doi.org/10.1016/j.chemosphere.2018.11.036.

Hu, Y., Zhao, Y., Zhao, X., Kumar, J.L.G., 2012. Comprehensive analysis of step-feeding strategy to enhance biological nitrogen removal in alum sludge-based tidal flow constructed wetlands. Bioresour. Technol. 111, 27–35. https://doi.org/10.1016/j.biortech.2012.01.165.

Hu, Y., Zhao, Y., Rymszewicz, A., 2014. Robust biological nitrogen removal by creating multiple tides in a single bed tidal flow constructed wetland. Sci. Total Environ. 470–471, 1197–1204. https://doi.org/10.1016/j.scitotenv.2013.10.100.

Hua, G., Salo, M.W., Schmit, C.G., Hay, C.H., 2016. Nitrate and phosphate removal from agricultural subsurface drainage using laboratory woodchip bioreactors and recycled steel byproduct filters. Water Res. 102, 180–189. https://doi.org/10.1016/j.watres.2016.06.022.

Huang, W., Gong, B., Wang, Y., Lin, Z., He, L., Zhou, J., He, Q., 2020. Metagenomic analysis reveals enhanced nutrients removal from low C/N municipal wastewater in a pilot-scale modified AAO system coupling electrolysis. Water Res. 173, 115530 https://doi.org/10.1016/j.watres.2020.115530.

Ji, Z., Tang, W., Pei, Y., 2022. Constructed wetland substrates: a review on development, function mechanisms, and application in contaminants removal. Chemosphere 286, 131564. https://doi.org/10.1016/j.chemosphere.2021.131564.

Ju, X., Wu, S., Zhang, Y., Dong, R., 2014. Intensified nitrogen and phosphorus removal in a novel electrolysis-integrated tidal flow constructed wetland system. Water Res. 59, 37–45. https://doi.org/10.1016/j.watres.2014.04.004.

Konneke, M., Bernhard, A.E., de la Torre, J.R., Walker, C.B., Waterbury, J.B., Stahl, D.A., 2005. Isolation of an autotrophic ammonia-oxidizing marine archaeon. Nature 437 (7058), 543–546. https://doi.org/10.1038/nature03911.

Li, C., He, Z.Y., Hu, H.W., He, J.Z., 2022. Niche specialization of comammox Nitrospira in terrestrial ecosystems: oligotrophic or copiotrophic? Crit. Rev. Environ. Sci. Technol. https://doi.org/10.1080/10643389.2022.2049578.

Li, J., Hu, Z., Li, F., Fan, J., Zhang, J., Li, F., Hu, H., 2019. Effect of oxygen supply strategy on nitrogen removal of biochar-based vertical subsurface flow constructed wetland: intermittent aeration and tidal flow. Chemosphere 223, 366–374. https://doi.org/10.1016/j.chemosphere.2019.02.082.

Li, J., Zheng, L., Ye, C., Ni, B., Wang, X., Liu, H., 2021a. Evaluation of an intermittent-aeration constructed wetland for removing residual organics and nutrients from secondary effluent: performance and microbial analysis. Bioresour. Technol. 329, 124897 https://doi.org/10.1016/j.biortech.2021.124897.

Li, M., Duan, R., Hao, W., Li, Q., Liu, P., Qi, X., Huang, X., Shen, X., Lin, R., Liang, P., 2021b. Utilization of elemental sulfur in constructed wetlands amended with granular activated carbon for high-rate nitrogen removal. Water Res. 195, 116996 https://doi.org/10.1016/j.watres.2021.116996.

Liu, C., Li, X., Yang, Y., Fan, X., Tan, X., Yin, W., Liu, Y., Zhou, Z., 2020. Double-layer substrate of shale ceramsite and active alumina tidal flow constructed wetland enhanced nitrogen removal from decentralized domestic sewage. Sci. Total Environ. 703, 135629 https://doi.org/10.1016/j.scitotenv.2019.135629.

Liu, M., Wu, S., Chen, L., Dong, R., 2014. How substrate influences nitrogen transformations in tidal flow constructed wetlands treating high ammonium wastewater? Ecol. Eng. 73, 478–486. https://doi.org/10.1016/j.ecoleng.2014.09.111.

Lu, S., Sun, Y., Lu, B., Zheng, D., Xu, S., 2020. Change of abundance and correlation of nitrospira inopinata-like comammox and populations in nitrogen cycle during different seasons. Chemosphere 241, 125098. https://doi.org/10.1016/j.chemosphere.2019.125098.

Pan, K.L., Gao, J.F., Fan, X.Y., Li, D.C., Dai, H.H., 2018. The more important role of archaea than bacteria in nitrification of wastewater treatment plants in cold season despite their numerical relationships. Water Res. 145, 552–561. https://doi.org/10.1016/j.watres.2018.08.066.

Pang, Q., Xu, W., He, F., Peng, F., Zhu, X., Xu, B., Yu, J., Jiang, Z., Wang, L., 2022. Functional genera for efficient nitrogen removal under low C/N ratio influent at low temperatures in a two-stage tidal flow constructed wetland. Sci. Total Environ. 804, 150142 https://doi.org/10.1016/j.scitotenv.2021.150142.

Pang, Y., Zhang, Y., Yan, X., Ji, G., 2015. Cold temperature effects on long-term nitrogen transformation pathway in a tidal flow constructed wetland. Environ. Sci. Technol. 49 (22), 13550–13557. https://doi.org/10.1021/acs.est.5b04002.

Pishgar, R., Dominic, J.A., Sheng, Z., Tay, J.H., 2019. Denitrification performance and microbial versatility in response to different selection pressures. Bioresour. Technol. 281, 72–83. https://doi.org/10.1016/j.biortech.2019.02.061.

Prakash, O., Green, S.J., Jasrotia, P., Overholt, W.A., Canion, A., Watson, D.B., Brooks, S. C., Kostka, J.E., 2012. Rhodanobacter denitrificans sp. nov., isolated from nitrate-rich zones of a contaminated aquifer. Int. J. Syst. Evol. Microbiol. 62 (Pt 10), 2457–2462. https://doi.org/10.1099/ijs.0.035840-0.

Roots, P., Wang, Y., Rosenthal, A.F., Griffin, J.S., Sabba, F., Petrovich, M., Yang, F., Kozak, J.A., Zhang, H., Wells, G.F., 2019. Comammox Nitrospira are the dominant ammonia oxidizers in a mainstream low dissolved oxygen nitrification reactor. Water Res. 157, 396–405. https://doi.org/10.1016/j.watres.2019.03.060.

Roth, J.J., Passig, F.H., Zanetti, F.L., Pelissari, C., Sezerino, P.H., Nagalli, A., Carvalho, K. Q., 2021. Influence of the flooded time on the performance of a tidal flow constructed wetland treating urban stream water. Sci. Total Environ. 758, 143652 https://doi.org/10.1016/j.scitotenv.2020.143652.

Saeed, T., Miah, M.J., Khan, T., Ove, A., 2020. Pollutant removal employing tidal flow constructed wetlands: media and feeding strategies. Chem. Eng. J. 382, 122874 https://doi.org/10.1016/j.cej.2019.122874.

Shi, P., Jiang, Y., Zhu, H., Sun, D., 2017. Impact of steel slag on the ammonium adsorption by zeolite and a new configuration of zeolite-steel slag substrate for constructed wetlands. Water Sci. Technol. 76 (3), 584–593. https://doi.org/10.2166/wst.2017.232.

Sorokin, D.Y., Lücker, S., Daims, H., 2018. Nitrolancea. In: Bergey's Manual of Systematics of Archaea and Bacteria, pp. 1–6. https://doi.org/10.1002/9781118960608.gbm01563.

Spring, S., Jackel, U., Wagner, M., Kampfer, P., 2004. Ottowia thiooxydans gen. nov., sp. nov., a novel facultatively anaerobic, N2O-producing bacterium isolated from activated sludge, and transfer of Aquaspirillum gracile to Hylemonella gracilis gen. nov., comb. nov. Int. J. Syst. Evol. Microbiol. 54 (Pt 1), 99–106. https://doi.org/10.1099/ijs.0.02727-0.

Sun, H., Jiang, T., Zhang, F., Zhang, P., Zhang, H., Yang, H., Lu, J., Ge, S., Ma, B., Ding, J., Zhang, W., 2021. Understanding the effect of free ammonia on microbial nitrification mechanisms in suspended activated sludge bioreactors. Environ. Res. 200, 111737 https://doi.org/10.1016/j.envres.2021.111737.

Su, Y., Wang, W., Wu, D., Huang, W., Zhu, G., 2018. Stimulating ammonia oxidizing bacteria (AOB) activity drives the ammonium oxidation rate in a constructed wetland (CW). Sci. Total Environ. 624, 87–95. https://doi.org/10.1016/j.scitotenv.2017.12.084.

Tan, X., Yang, Y., Liu, Y., Li, X., Fan, X., Zhou, Z., Liu, C., Yin, W., 2019. Enhanced simultaneous organics and nutrients removal in tidal flow constructed wetland using activated alumina as substrate treating domestic wastewater. Bioresour. Technol. 280, 441–446. https://doi.org/10.1016/j.biortech.2019.02.036.

Tang, C., Zhao, Y., Kang, C., He, J., Yang, Y., Morgan, D., 2021. Creating tidal flow via siphon for better pollutants removal in a microbial fuel cell-constructed wetland. J. Environ. Manag. 290, 112592 https://doi.org/10.1016/j.jenvman.2021.112592.

Vymazal, J., 2007. Removal of nutrients in various types of constructed wetlands. Sci. Total Environ. 380 (1–3), 48–65. https://doi.org/10.1016/j.scitotenv.2006.09.014.

Wang, M., Huang, G., Zhao, Z., Dang, C., Liu, W., Zheng, M., 2018. Newly designed primer pair revealed dominant and diverse comammox amoA gene in full-scale wastewater treatment plants. Bioresour. Technol. 270, 580–587. https://doi.org/10.1016/j.biortech.2018.09.089.

Wang, X.Y., Liu, L.T., Lin, W.T., Luo, J.F., 2020. Development and characterization of an aerobic bacterial consortium for autotrophic biodegradation of thiocyanate. Chem. Eng. J. 398, 125461 https://doi.org/10.1016/j.cej.2020.125461.

Wang, Z., Huang, M., Qi, R., Fan, S., Wang, Y., Fan, T., 2017. Enhanced nitrogen removal and associated microbial characteristics in a modified single-stage tidal flow constructed wetland with step-feeding. Chem. Eng. J. 314, 291–300. https://doi.org/10.1016/j.cej.2016.11.060.

Xu, D., Ling, H., Li, Z., Li, Y., Chen, R., Cai, S., Gao, B., 2022. Treatment of ammonium-nitrogen–contaminated groundwater by tidal flow constructed wetlands using different substrates: evaluation of performance and microbial nitrogen removal pathways. Water Air Soil Pollut. 233 (5), 1–13. https://doi.org/10.1007/s11270-022-05633-6.

Xu, R., Zhang, Y., Liu, R., Cao, Y., Wang, G., Ji, L., Xu, Y., 2019. Effects of different substrates on nitrogen and phosphorus removal in horizontal subsurface flow constructed wetlands. Environ. Sci. Pollut. Res. Int. 26 (16), 16229–16238. https://doi.org/10.1007/s11356-019-04945-1.

Xu, S., Wang, B., Li, Y., Jiang, D., Zhou, Y., Ding, A., Zong, Y., Ling, X., Zhang, S., Lu, H., 2020. Ubiquity, diversity, and activity of comammox Nitrospira in agricultural soils. Sci. Total Environ. 706, 135684 https://doi.org/10.1016/j.scitotenv.2019.135684.

Zhan, X., Yang, Y., Chen, F., Wu, S., Zhu, R., 2020. Treatment of secondary effluent by a novel tidal-integrated vertical flow constructed wetland using raw sewage as a carbon source: contribution of partial denitrification-anammox. Chem. Eng. J. 395, 125–165. https://doi.org/10.1016/j.cej.2020.125165.

Zhang, Q., Yang, Y., Chen, F., Zhang, L., Ruan, J., Wu, S., Zhu, R., 2021. Effects of hydraulic loading rate and substrate on ammonium removal in tidal flow constructed wetlands treating black and odorous water bodies. Bioresour. Technol. 321, 124468 https://doi.org/10.1016/j.biortech.2020.124468.

Zhao, L., Fu, G., Pang, W., Tang, J., Guo, Z., Hu, Z., 2022. Biochar immobilized bacteria enhances nitrogen removal capability of tidal flow constructed wetlands. Sci. Total Environ. 836, 155728 https://doi.org/10.1016/j.scitotenv.2022.155728.

Zhao, Z., Huang, G., He, S., Zhou, N., Wang, M., Dang, C., Wang, J., Zheng, M., 2019. Abundance and community composition of comammox bacteria in different ecosystems by a universal primer set. Sci. Total Environ. 691, 146–155. https://doi.org/10.1016/j.scitotenv.2019.07.131.

Zhi, W., Ji, G., 2014. Quantitative response relationships between nitrogen transformation rates and nitrogen functional genes in a tidal flow constructed wetland under C/N ratio constraints. Water Res. 64, 32–41. https://doi.org/10.1016/j.watres.2014.06.035.

Zuo, M., Renman, G., Gustafsson, J.P., Klysubun, W., 2018. Dual slag filters for enhanced phosphorus removal from domestic waste water: performance and mechanisms. Environ. Sci. Pollut. Res. Int. 25 (8), 7391–7400. https://doi.org/10.1007/s11356-017-0925-y.